Local anisotropy of muon flux during Forbush decreases from URAGAN data

Journal of Physics: Conference Series **632** (2015) 012049 doi:10.1088/1742-6596/632/1/012049

Local anisotropy of muon flux during Forbush decreases from URAGAN data

N Barbashina[1], N Ampilogov[1], I Astapov[1], V Borog[1], A Dmitrieva[1], A Kovylyaeva[1], R Kokoulin[1], K Kompaniets[1], G Mannocchi[2], Yu Mishutina[1], A Petrukhin[1], O Saavedra[3], V Shutenko[1], O Sit'ko[1], G Trinchero[2], E Yakovleva[1], I Yashin[1]

[1]National Research Nuclear University MEPhI (Moscow Engineering Physics Institute), 115409 Moscow, Russia
[2]Istituto di Fisica dello Spazio Interplanetario, INAF, 10133 Torino, Italy
[3]Dipartimento di Fisica dell' Universita di Torino and INFN, 10125 Torino, Italy

E-mail: NSBarbashina@mephi.ru

Abstract. The approach to the analysis of spatial-angular characteristics of the muon flux variations at different phases of Forbush decrease development according to the muon snapshots (muongraphies) obtained using muon hodoscope URAGAN, as well as the analysis results are presented.

Introduction

One of the perfect examples of the influence of solar activity on the cosmic rays is the Forbush effect (FE), which is a sharp decrease of CR intensity due to the propagating large-scale solar wind disturbances [1], and, therefore, is often called a Forbush decrease (FD). Study of the FD using the muon flux has the following features: the first, muons are more sensitive to higher energies of primary cosmic rays (PCR) than neutrons, and so allow study heliospheric disturbances responsible for the high-energy PCR modulation; the second and more important, muons retain the primary particle direction and this enables to obtain the spatial and angular picture of modulations of cosmic rays in the near-Earth space and to study their dynamics in a wide range of zenith and azimuth angles using a single muon hodoscope. In this paper we consider anisotropy of muon flux on the observation level only, since all necessary calculations for transition from muon energy and direction to primary proton energy and direction were made earlier. In paper [2] the mean and median energies of primary particle in dependence to the zenith angle were calculated. These values were used for the calculations of asymptotic directions [3]. The samples of transition of the local muon flux distribution for the Moscow location point (55.7º N, 37.7º E, 173 m a.s.l.) to the primary proton distribution at the boundary of magnetosphere presented in the GSE system were given in our other papers (see f. e. [4]). But our investigations have shown that many features of helispherical processes can be studied in a local system.

Muon hodoscope URAGAN (URAGAN) [5] operates as a part of the unique scientific facility NEVOD [6] since 2006. Hodoscope consists of four supermodules (SMs) with high spatial and angular accuracy of muon registration and registers muon flux variations both in the integral mode and in the hodoscopic mode, i.e. when the variations of the muon flux from different directions of the

celestial hemisphere are measured simultaneously. The main feature of the muon hodoscope technique is the real time reconstruction of muon trajectories that can be distributed in the cells of angular matrix of any type. The analysis of these matrices enables to study zenith-angular and azimuthal dependences, as well as the muon flux anisotropy. A similar approach was used in the narrow angle muon telescope at the Mt. Norikura [7], but with lower angular accuracy (about 7°) in comparison with the URAGAN (about 1°). The advantage of the considered approach can be illustrated by the comparison with the multidirectional muon telescopes (MMT) combined in the Global Muon Detector Network (GMDN) [8]. MMT register integral muon flux in rather wide and fixed intervals of zenith and azimuthal angles which, in addition, are overlapped [9]. In the contrast with the GMDN, the muon hodoscope enables to obtain practically differential distributions on zenith and azimuthal angles of arriving muons.

Every minute one SM of the URAGAN registers about 80,000 muons and records their arrival directions in two-dimensional angular matrices. To analyze the muon flux intensity variations during the FD, the matrices averaged over the data of three supermodules obtained during one hour expositions are used. The statistical reliability of every matrix is about 15 million events. Sequence of such matrices-snapshots (muongraphies) provides information about variations in spatial and angular distributions of the muon flux intensity during the FD. The FDs registered by the URAGAN in the period from 2007 to 2012 are analyzed in the paper. Over this period 185 FDs were observed by the integral counting rate. Among them, 44 FDs with amplitude > 0.5%, which are well separated and do not overlap with each other, were selected. To estimate the FD amplitude, the 10-minute data on the muon flux integral intensity corrected for the barometric and temperature effects were used [10, 11]. To study the muon flux relative anisotropy, the muon snapshots and quantitative parameters describing them were used. Each analyzed event was divided into different phases: before the decrease beginning (24 hours), phases of decrease, minimum and recovery (not more than 24 hours).

2. Experimental data and analysis technique

Experimental data obtained with the supermodules of the URAGAN setup are binary files that contain information about one minute snapshots. Supermodule response represents the information on strips triggered in each of two projection planes *XZ* and *YZ*. Track parameters (two projection angles) are reconstructed in real time mode by the software which is based on histogramming of the hits in each projection plane. Projection angles are accumulated in three types of two-dimensional matrices (θ, φ), (θ_X, θ_Y) and ($tg\theta_X$, $tg\theta_Y$) during the minute interval. Different matrices are used to solve various tasks.

To analyze the muon flux intensity variations during the FD, the hourly matrices ($tg\theta_X$, $tg\theta_Y$) summed over three SM are used. Each matrix (figure 1 a) is normalized to the average matrix obtained by averaging minute matrices for the last day (figure 1 b). The result is a matrix (figure 1 c), each bin of which contains deviations from the average one in units of their rms values (σ). To smooth sharp fluctuation peaks in separate bins, all values of the matrix are smoothed using the Gaussian filter (figure 1 d). To optimize the presentation of information considering low statistics in the matrix corners, it is reasonable to present it in the form of a circle limited by zenith angle of 75° (figure 1 e). Such matrix is a "muon snapshot" of the upper hemisphere bounded by the aperture of the detector.

Thin lines in figure 1 e show N-S and E-W directions. Circles highlight zenith angles of 30°, 45°, 60° and 75°. Statistical reliability of such matrix is about 5 million events. The scale in the upper right corner of figure 1 e shows the deviation from the average in sigma, red color corresponds to the excess of muons, blue color – to the deficit of muons. Additionally, for each matrix the following auxiliary information is displayed: the beginning and the end of the snapshot exposure; average atmospheric pressure in the analyzed time interval; matrix type (in this case, the matrix of projection angle tangents) and the value of deviation from the average integral intensity (δ); length of the horizontal projection of the muon flux relative local anisotropy vector (*r*, relative to the normalization and divided by the statistical error) and its direction (φ_r) indicating the muon flux increase.

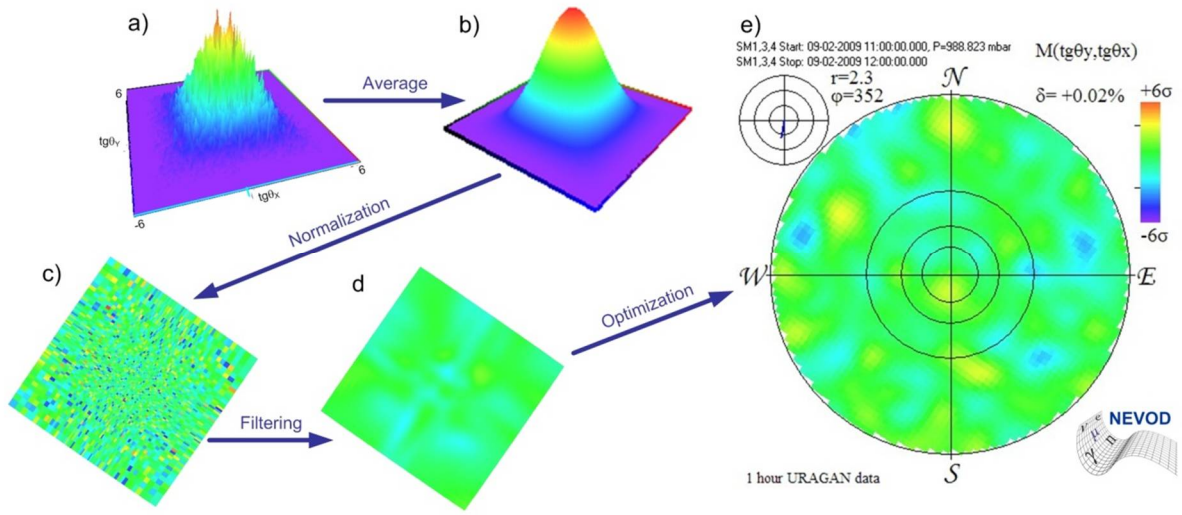

Figure 1. Angular distribution of muons registered during one minute (the matrix of tangents of projection angles): a) initial matrix; b) after averaging; c) two-dimensional image after normalization; d) smoothed angular matrix; e) resulting angular matrix.

Local anisotropy vector $\vec{A}$ characterizes the zenith-azimuthal distribution of the muon flux during some period of time and represents the sum of unit vectors normalized to the number of events [3]. The direction of each unit vector is obtained at a single muon track reconstruction. The summarized vector indicates the average direction of the muon flux. For calculations, the matrix (θ, φ) with the cell dimensions of 1° for zenith (θ) and 4° for azimuthal (φ) angles are used. The vector can be expanded in directions. Particularly, in this work the projections on the geographic South (A_S) and East (A_E) were used. To study the deviations from the mean direction of the anisotropy vector, the relative anisotropy vector $\vec{r}$ and its projections to the South (r_S) and East (r_E) were used:

$$\vec{r} = \vec{A} - \left\langle \vec{A} \right\rangle,$$

$$r_S = A_S - \left\langle A_S \right\rangle \text{ and } r_E = A_E - \left\langle A_E \right\rangle,$$

where $\left\langle \vec{A} \right\rangle$ is the average anisotropy vector calculated for a long period of time. Vector $\vec{r}$ and its projections to the South and East indicate the direction of the maximum of muon flux variations. Correspondingly, minimum is on the opposite side. Projections of the vectors r_S and r_E are calculated in geographic coordinates. For the primary protons (considering asymptotic trajectories) the geographical directions N-S and W-E correspond to the asymptotic directions E-W and N-S, respectively. These quantities are convenient for the study of the regularities in the muon flux anisotropy variations on the azimuthal direction during the FD and of the correlation between them for the quantitative description of the muon flux angular distribution variations (for the description of the muon snapshots) [12-14].

3. Examples and results of the analysis of the muon flux relative anisotropy variations

For each phase of 44 selected FDs the muon snapshots and correlations between the projections of the vector $\vec{r}$ to the South and East (r_S and r_E) were plotted.

For example, figure 2 shows the muon snapshots for the FD on October 24, 2011. This is a large enough decrease of the counting rate which was observed in many neutron monitors. According to the data of the URAGAN and the Moscow Neutron Monitor [15], its amplitude was about 1.5% and 4.5%, respectively. Each row of the snapshots in figure 2 corresponds to the different phase of the FD development: the first row reflects the period before the beginning of Forbush decrease (24/10/2011

8:00 – 24/10/2011 18:00, every 3 hours); the second, phase of decrease (24/10/2011 20:00– 25/10/2011 6:00, every 3 hours); then, phase of minimum (25/10/2011 7:00– 25/10/2011 17:00, every 3 hours); the last row corresponds to the phase of recovery (25/10/2011 18:00– 26/10/2011 13:00, every 6 hours).

In figure 2, the muon flux variations at different angles during the FD are clearly seen. At the first phase of the FD, the increase of the counting rate in the range of zenith angles from 0 to 45 degrees, which damps before the FD beginning, is observed. At the phase of decrease and minimum, the muon counting rate decrease begins in the same range of zenith angles, but with the N-E azimuth displacement. By 5:00 on 25/10/2011, the counting rate decrease spread on the particles registered under zenith angles more than 60°. At the phase of minimum, the decrease of the flux of registered particles was revealed also in a wide range of zenith angles from 0 to 60 degrees. At the recovery phase the counting rate was changed from S-W decreasing to S-E increasing.

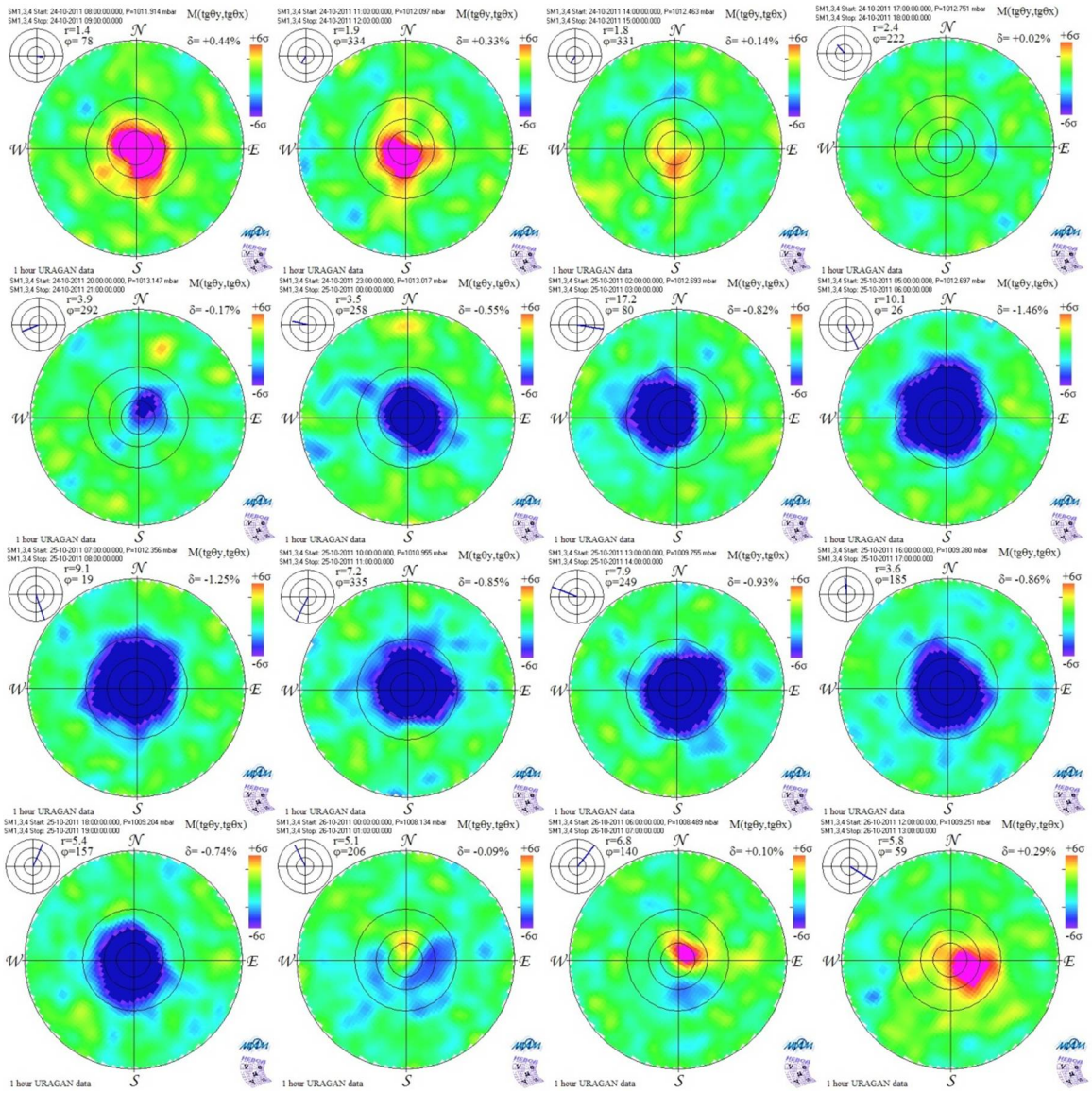

Figure 2. Muon snapshots of FD on October 24, 2011.

Correlations between the projections of the relative anisotropy vector r_S and r_E during the FD on October 24, 2011 are shown in figure 3. Circles in the graphs corresponds to the r_S and r_E variation limits equal to 0.52×10^{-3} during the quiet period from 7 to 10 of February 2009 which is characterized by the absence of disturbances in the heliosphere and the Earth's magnetosphere. The rms values of r_S and r_E during this period are $\sigma(r_S) = 1.30\times10^{-4}$ and $\sigma(r_E) = 1.28\times10^{-4}$, respectively. Thus, the exceedance of the circle boundaries corresponds to the 4σ exceedance of the r_S and r_E variations.

As seen from the figure 3, during the first FD phase the relative anisotropy variations are not observed. At the other phases, the excess of the muon flux relative anisotropy is seen in comparison with the normal value: at the phase of decrease it predominates in the E-W azimuthal direction, at the phase of minimum it moves from the South to the North, at the phase of recovery it shifts to the geographical North.

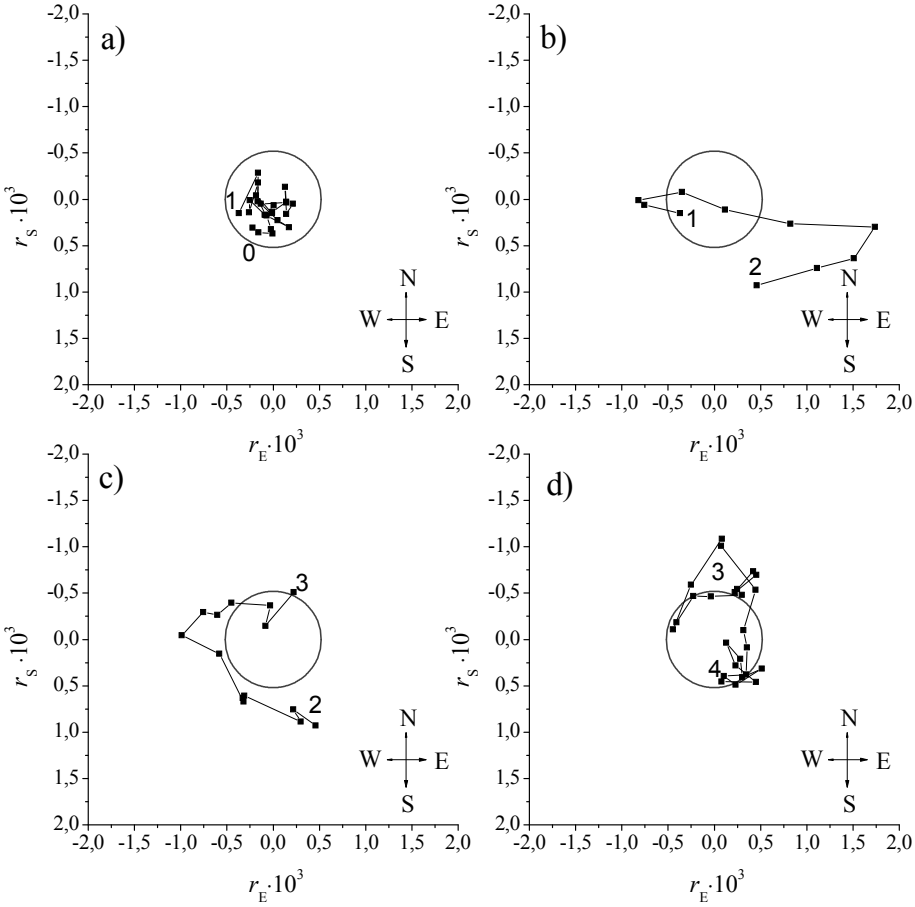

Figure 3. Correlations between r_S and r_E for the FD on October 24, 2011 at four phases of the event development: (a) 0 – 23/10/2011 20:00, 1 – 24/10/2011 20:00; (b) 1 – 24/10/2011 20:00, 2 – 25/10/2011 5:00 UT; (c) 2 – 25/10/2011 5:00, 3 – 25/10/2011 18:00 UT; (d) 3 – 25/10/2011 18:00 UT, 4 – 26/10/2011 18:00 UT.

The analysis of 44 FDs showed that the relative anisotropy exceeding the r_S and r_E variations more than 4σ is observed: at all phases of 12 FDs, at three phases of 11 FDs, at two phases of 7 FDs, at one phase of 6 FDs, and is absent at all phases of 8 FDs. The study of each phase separately showed that the significant relative anisotropy is observed: in the period before FD in 25 FDs, at the phase of decrease in 27 FDs, at the phase of minimum in 25 FDs, at the phase of recovery in 24 FDs. To study the regularities in the behavior of the relative anisotropy along the N-S and E-W geographical directions, the distributions of hourly values of the r_S and r_E for all phases of FDs (figure 4, top and bottom) normalized to the number of points at each phase were plotted.

Distributions of the r_S and r_E values before the FD beginning are symmetrical and are mainly in the range from -1.0×10^{-3} to 1.0×10^{-3}. At the phase of decrease a wider range for both parameters is observed: $r_S = (-1.2 \div 2.0)\times10^{-3}$ and $r_E = (-1.7 \div 1.7)\times10^{-3}$. At that, the values of r_S are obviously shifted towards the South: $\langle r_S \rangle = (0.18 \pm 0.02)\times10^{-3}$. This means that the minimum of the flux is observed more frequently from the North which, in its turn, corresponds to the asymptotic East. At the phase of minimum $r_S = (-1.3 \div 1.0)\times10^{-3}$ and $r_E = (-1.2 \div 1.0)\times10^{-3}$, the mean values practically coincide, r_S is shifted more towards the North. At the recovery phase, the distributions of the relative anisotropy parameters are almost symmetrical.

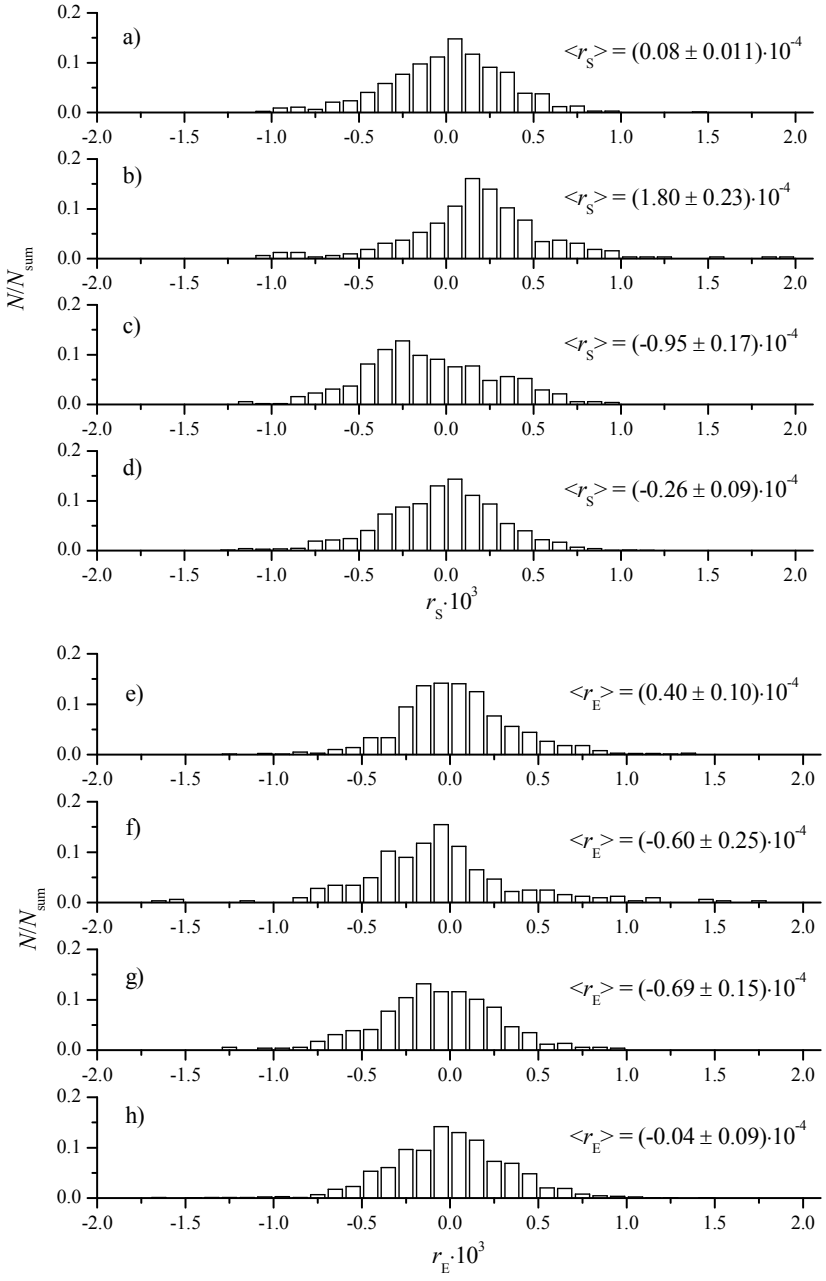

Figure 4. Distribution of values of r_S (top) and r_E (bottom) parameters at four FD phases: (a) and (e) – before the FD beginning; (b) and (f) – phase of decrease; (c) and (g) – phase of minimum; (d) and (h) – phase of recovery.

Thus, on average, at the phase of the counting rate decrease during the FD, the muon flux from the geographic South decreases weaker than from the North, at the phase of minimum vice versa, which corresponds to the variation of the E-W anisotropy of primary cosmic rays. At the other phases, the relative anisotropy is almost symmetrical.

4. Conclusions

Muon hodoscope URAGAN allows reconstruct trajectories of the detected particles with high angular and spatial accuracy and obtain muon snapshots (muongraphies). Such snapshots give qualitative information about the dynamics of the decrease or increase of the intensity of the muon flux from different directions. Usage of the correlations between the projections r_E and r_S of the relative anisotropy vector allows quantitative studying of temporal variations of the muon flux anisotropy at different phases of the FD development. The analysis of 44 Forbush decreases registered by the URAGAN showed that the changes in the relative anisotropy of the muon flux variations are observed mainly at the phases of decrease and minimum and, on the average, correspond to the E-W primary cosmic ray anisotropy variation.

Acknowledgments

This work was performed at the NEVOD Scientific and Educational Center with the financial support from the State provided by the Russian Ministry of Education and Science (government task and project No. RFMEFI59114X0002) and the grant of the Leading Scientific School NSh-4930.2014.2.

References

[1] Belov A V *et al* 2001 *Izv. RAN. Ser. Fiz.* **65** 373
[2] Yakovleva E I *et al* 2009 *Bull. Russ. Acad. Sci. Phys.* **73** *357*
[3] Shutenko V V *et al* 2009 *Bull. Russ. Acad. Sci. Phys.* **73** *347*
[4] Yashin I I et al. 2013 J. Phys.: Conf. Ser. **409** 012192
[5] Barbashina N S *et al* 2008 *Instrum. Experim. Techn.* **51** 180
[6] Unique scientific facility NEVOD: http://ununevod.mephi.ru/en/
[7] Fujimoto K *et al* 2001 *Proc. 27th ICRC (Hamburg, Germany)* **9** 3523
[8] Rockenbach M *et al* 2014 *Space Sci. Rev.* **182**, 1
[9] Yasue S *et al* 2003 *Proc. 28th ICRC (Tsukuba, Japan)* **6** 3461.
[10] Barbashina N S *et al* 2009 *Bull. Russ. Acad. Sci. Phys.* **73** 343
[11] Dmitrieva A N *et al* 2011 *Astroparticle Physics* **34** 401
[12] Shutenko V.V. *et al* 2011 *Proc. 32nd ICRC (Beijing, China)* **11** 276
[13] Barbashina N.S. *et al* 2013 *Bull. Russ. Acad. Sci.: Phys*. **77** 532
[14] Shutenko V V *et al* 2013 *Geomagn. Aeronomy.* **53** 571
[15] Database of Moscow neutron monitor: http://cr0.izmiran.rssi.ru/mosc/main.htm